# The Interpanel Gap Scattering Effect in a Compact Range

Reuven Shavit, *Senior Member, IEEE,* Adam P. Smolski, and Crit J. Cook, *Member, IEEE*

***Abstract*—In recent years, the compact range has become a popular measurement tool in the evaluation of microwave antennas. This trend leads to the use of larger reflectors over larger frequency bands. Those reflectors can be built to the required accuracies, but they have to be assembled from many panels which introduce interpanel gaps. The electromagnetic scattering produced by the gaps affects the uniformity of the field in the quiet zone of the compact range. An analytical approach coupled with experimental determination of a key parameter has been developed to quantify the effect of the scattering from the interpanel gaps in a compact range. The results show the significance of this effect on the copol and x-pol distribution in the quiet zone area.**

## I. Introduction

THE uniformity of the field in a compact range quiet zone area is determined by many factors, like the edge diffraction from the reflector rim, the stray signals transmitted by the feed and the surface accuracy of the reflector. All these factors have been extensively considered in the literature and effective optimization methods have been proposed. This paper will concentrate only on the scattering effect of the interpanel gaps, which will be characterized by equivalent radiating linear magnetic currents. The analysis requires as a first step to determine the scattering effect of a single gap and then superimpose the multiple gap effect. The single gap scattering has been considered analytically by Kabalan [1], [2], who solved the problem of the scattered field from an infinite gap illuminated by an incident transverse electric (TE) or transverse magnetic (TM) polarized field. The electric field integral equation (EFIE) was formulated and solved with the method of moments (MM). Miller [3] solved the same problem but with the geometrical theory of diffraction (GTD) approach. Recently, Senior [4] considered the scattering from a filled gap by formulating its integral equation and solving it by MM.

In the present analysis, we have introduced an experimental new parameter, the magnetic induced field ratio (MIFR), which characterizes the complex amplitude of the scattered field in the gap.

This parameter combined with *a priori* knowledge of the field distribution in the gap determines the full scattering characteristics from the gap. This is an alternative approach to the direct analytical approach suggested by MM and GTD. The advantage of this quasi-empirical concept is its relative simplicity and its flexibility to characterize the scattering from any type of gap without extensive computational effort as required by the other methods. However, it requires *a priori* knowledge of the field distribution in the gap.

The multiple gap scattering effect in the quiet zone area has been considered by Black [5] for a parallel gap geometry in a parabolic cylinder. This work considers such an effect but for an offset parabolic reflector and for an arbitrary geometry of gaps. The result of this analysis is the perturbed copol and x-pol electric field in the quiet zone area.

Manuscript received December 29, 1989; revised September 7, 1990.

The authors are with Electronic Space Systems Corporation, Old Powder Mill Road, Concord, MA 01742-4697.

IEEE Log Number 9041786.

## II. Formulation

Fig. 1 shows the geometry of an offset parabolic reflector fed by a $y$-polarized linear feed and the $q$th gap out of a total of $Q$ gaps. The focal distance of the paraboloidal reflector is $f$ and the distance from the aperture to the quiet zone is $z_f$. The feed is tilted an angle $\theta_0$ toward the reflector center and its local coordinates are $(x', y', z')$. The global coordinates of the main reflector are $(x, y, z)$ and its projected diameter on the $x$-$y$ plane is $D$. The local coordinates of the center of the $q$th gap are $(x'', y'', z'')$. Its projected length on the main reflector aperture is $l_q$, its width $W_q$, and its inclination with respect to the $x$ axis is $\delta_q$.

The first step in the analysis would be to evaluate the unperturbed field distribution $\mathbf{E}_{\text{up}}$ in the quiet zone area for a main reflector without gaps. If we follow Chu's [6] analysis based on physical optics and assume a symmetric feed with a pattern $e_i(\theta')$, one can compute $\mathbf{E}_{\text{up}}$,

$$\mathbf{E}_{\text{up}} = \frac{e^{-j\psi_0}}{2f}\left[N\mathbf{1}_x + M\mathbf{1}_y\right] \tag{1}$$

in which $\psi_0$ is a constant phase from the antenna aperture to the quiet zone and $M$ and $N$ are the co-polarization and cross-polarization components of the field:

$$M = e_i(\theta')\left[\sin\theta'\cos\phi'\sin\theta_0 - \sin^2\phi'(\cos\theta' + \cos\theta_0) - \cos^2\phi'(1 + \cos\theta'\cos\theta_0)\right] \tag{2}$$

$$N = e_i(\theta')\sin\phi'\left[\sin\theta'\sin\theta_0 - \cos\phi'(1 - \cos\theta')(1 - \cos\theta_0)\right]. \tag{3}$$

The $q$th gap is illuminated by the feed which can be regarded as a point source with a pattern $e_i(\theta')$.

The tangential field excited in the gap has two components parallel and perpendicular to the gap axis. Since the propagation direction of the incident field is not normal to the gap axis, a traveling wave is excited in the gap. This wave determines the peak scattering angle from the gap which coincides with the angle of the reflected collimated beam from the main reflector. This assumption enables one to project the gaps on the main reflector aperture, and their peak scattering direction would be $z$ directed.

We call the ratio of the actual field excited in the gap to the tangential incident field in the gap the MIFR. Since the electric field in the gap has two components parallel and perpendicular to its axis, we introduce two MIFR's parallel to the gap axis $g_{\parallel}$ (TM case) and perpendicular $g_{\perp}$ (TE case). Rusch [8] and

0018-926X/91/0400-0480$01.00 

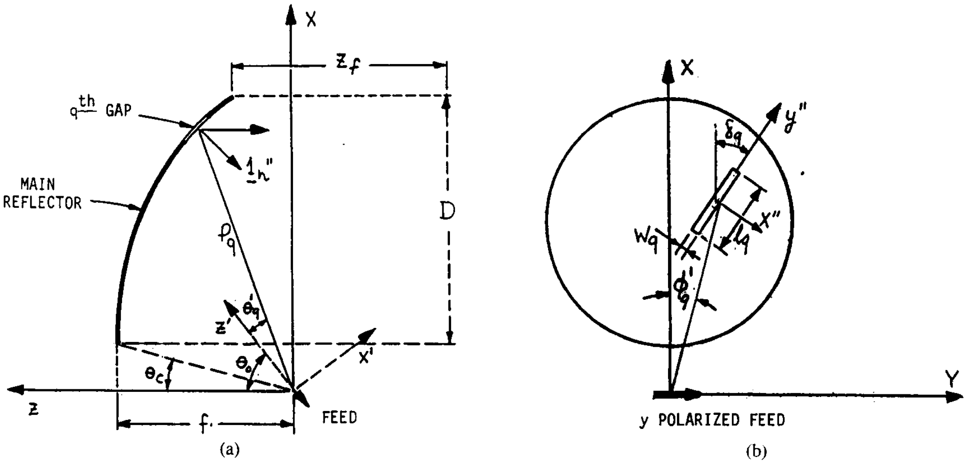


Fig. 1. The geometry of the compact range with a gap. (a) Side view. (b) Front view.

Kennedy [9] derived the induced field ratio (IFR) expression for cylindrical metal and dielectric beams. We applied the same concept to magnetic currents and obtained an analytical expression for the MIFR. In the TE case,

$$g_{\perp} = -\frac{1}{2W\cos\theta_0\eta H_0}\int_{S_1} Jms(x)\,dx \tag{4}$$

in which $\theta_0$ is the incident angle, $W$ is the gap width, $\eta = \sqrt{\mu/\epsilon}$, $k = \omega\sqrt{\mu\epsilon}$, $H_0$ is the incident magnetic field, $S_1$ denotes the integration path across the gap and $Jms$ is the equivalent magnetic current in the gap.

Similarly, for the TM case:

$$g_{\|} = \frac{1}{2W\cos\theta_0 E_0}\int_{S_1} Jms(x)\,dx \tag{5}$$

where $E_0$ is the incident electric field. Kabalan [1], [2] derived an approximate analytical expression for the magnetic current induced in a narrow gap ($W < 0.1\ \lambda$). For the TE case, the expression is

$$Jms(x) = \left[\frac{j}{\nu + ln\left(\frac{kw}{8}\right) + j\frac{\pi}{2}} - kx\sin\theta\right] \cdot \frac{H_0\eta}{k\sqrt{(W/2)^2 - X^2}} \tag{6}$$

in which $\nu = 0.5772$ is the natural algorithm of Euler's constant and $X$ is the transverse coordinate to the gap axis. A similar expression exists for the TM case:

$$Jms(x) = jE_0\frac{k\cos\theta}{2}(-2 + jkx\sin\theta)\cdot\sqrt{(W/2)^2 - X^2}. \tag{7}$$

Substitution of (6) and (7) into (4) and (5) gives the MIFR. A plot of the calculated $g_{\|}$ and $g_{\perp}$ under the above assumptions is shown in Fig. 3. Based on Kabalan's [1], [2] analysis we assume for the scattering analysis from the gaps that the field distribution excited across the projected gaps is constant for the perpendicular component and has a cosinusoidal dependence for the axial component. This assumption holds well for relatively narrow gaps ($W \ll \lambda$) and is a good approximation (for radiation calculations) to the approximate analytical results presented in (6) and (7). By the Schelkunoff equivalence principle, the surface equivalent magnetic current induced in the gap would be

$$\mathbf{J}_{ms}^q = -2\mu_0^{-1}\mathbf{1}_{n''}x\left[E_{x''}^q\mathbf{1}_{x''} + E_{y''}^q\mathbf{1}_{y''}\right] \tag{8}$$

in which

$$E_{x''}^q = g_{\perp}\left(-E_{i,x}^q\sin\delta_q + E_{i,y}^q\cos\delta_q\right) \tag{9}$$

$$E_{y''}^q = g_{\|}\cos\frac{\pi x''}{W_q}\left(E_{i,x}^q\cos\delta_q + E_{i,y}^q\sin\delta_q\right). \tag{10}$$

$E_{i,x}^q$ and $E_{i,y}^q$ are the $x$ and $y$ components of the incident field from the feed at the center of the $q$th gap and $\mathbf{1}_{n''}$, $\mathbf{1}_{x''}$, $\mathbf{1}_{y''}$ are unit vectors as shown in Fig. 1. In the derivation of (8), we made the assumption that the $q$th gap is projected on to the main reflector aperture. Such an assumption holds if we look to radiation angles close to boresight.

Given the equivalent magnetic current of the $q$th gap, one can compute its radiated field. Accordingly, the scattered copol component of the $q$th gap in the quiet zone plane would be

$$E_{\text{copol}}^q(x, y, z_f) = \frac{jk\cos\theta_q''}{2\pi z_f}\left(E_{i,x}^q P_q + E_{i,y}^q Q_q\right) \tag{11}$$

where

$$P_q = \sin\delta_q\cos\delta_q\left(g_{\|}I_{\|}^q - g_{\perp}I_{\perp}^q\right) \tag{12}$$

$$Q_q = g_{\|}I_{\|}^q\sin^2\delta_q + g_{\perp}I_{\perp}^q\cos^2\delta_q. \tag{13}$$

Since the quiet zone is closer to the antenna aperture than the far-field criterion for the radiating gaps, $I_{\|}^q$ and $I_{\perp}^q$ are the Fresnel patterns [7] due to the axial and the transverse components of the equivalent magnetic currents induced in the $q$th gap. Similarly, one can derive the x-pol component of the $q$th gap,

$$E_{\text{xpol}}^q(x, y, z_f) = \frac{jk\cos\theta_q''}{2\pi z_f}\left(E_{i,x}^q R_q + E_{i,y}^q P_q\right) \tag{14}$$

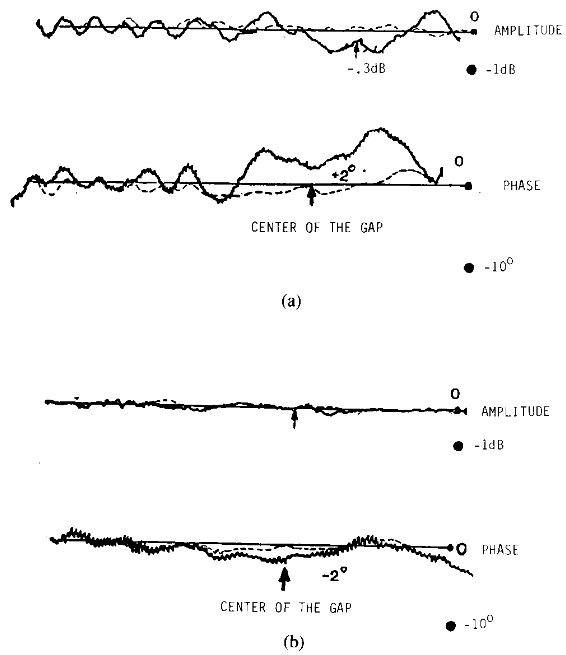


Fig. 2. Typical recorded signal throughout the panels movement with (——) and without (- - - -) a 5/16-inch wide gap for (a) horizontal and (b) vertical polarizations at 3 GHz.

where

$$R_q = g_{\parallel} I_{\parallel}^q \cos^2 \delta_q + g_{\perp} I_{\perp}^q \sin^2 \delta_q. \tag{15}$$

The single gap analysis can be extended to multiple gap configuration by superimposing the scattered fields of the individual gaps given by (11) and (14) over the unperturbed field given by (1). The total perturbed field in the quiet zone would be

$$\mathbf{E} = \mathbf{E}_{\text{up}} + \sum_{q=1}^{Q} \left( E_{\text{copol}}^q \mathbf{l}_y + E_{\text{xpol}}^q \mathbf{l}_x \right). \tag{16}$$

In the presented approach, it was assumed that the gaps are sufficiently separated so that at the frequency of interest, the mutual coupling among the gaps is negligible.

## III. Numerical and Experimental Results

The MIFR was measured in a test set up assembled for this purpose. A vertical gap was simulated in between two conductive flat panels. The panels with the gap were mounted on a positioner track and moved in front of transmitting and receiving horns. The transmitting horn boresight axis made an angle of 45° with the normal to the panels and was perpendicular to the gap axis, while the receiving horn was oriented to maximize the reception at the specular reflection from the panels. The amplitude and phase of the received signal was recorded throughout the panels movement. No significant change in the recorded signal was detected for lower incident angles. This result implies that the MIFR remains constant for low incident angles on the gaps. In practical reflector applications, the incident angle on the gap is less than 35°, therefore, the results are pertinent in these cases. The distance between the horns and the gap fulfilled the far-field criterion of the horns. Fig. 2 shows a typical signal recorded for (a) horizontal and (b) vertical polarizations. The test was conducted at 3 GHz for a gap 5/16-in wide. The reference signal is the specular reflection from the panels (dashed line), while the perturbation (fluctuation) is caused by the scattering from the gap (solid line). One can observe that the perturbation due to a horizontally polarized illuminating field is more significant than that due to a vertically polarized incident field. This fact can be explained by the different boundary conditions in the gap for the two polarizations.

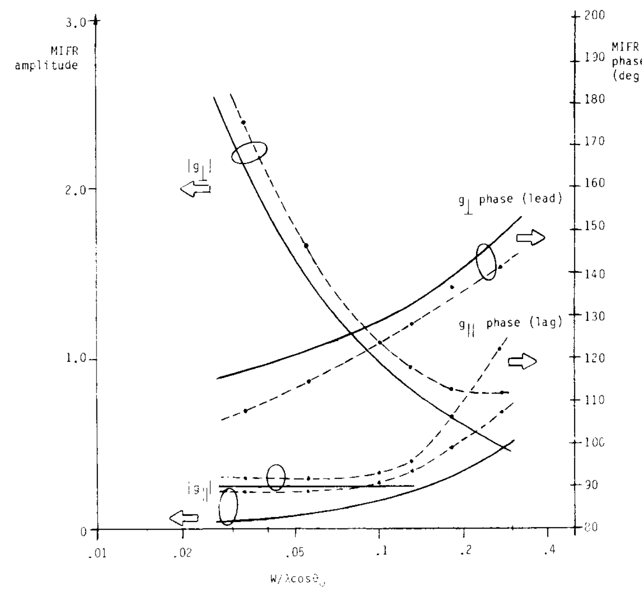


Fig. 3. Computed (——) and measured (- - - -) MIFR for an infinite slot in a conductive plane versus $W/\lambda \cdot \cos\theta_0$.

Given the change in amplitude and phase of the recorded signal from the tested gap, one can compute the MIFR based on Rusch's [8] formula,

$$g_{\parallel,\perp} = \left(10^{+0.05\Delta\alpha} e^{+j\Delta\phi} - 1\right) \frac{e^{-j45^0}}{W \cos\theta_0} \sqrt{\frac{\lambda \eta_0 \eta_0'}{\eta_0' + \eta_o}} \tag{17}$$

where

| | |
|---|---|
| $\Delta\alpha$[dB] | amplitude change due to the tested gap. |
| $\Delta\phi$[deg] | phase change due to the tested gap. |
| $W$ | width of the tested gap. |
| $\lambda$ | wavelength |
| $\eta_0$ | distance between the tested gap and the transmitting horn. |
| $\eta_0'$ | distance between the tested gap and the receiving horn |
| $\theta_0$ | incident angle on the gap. |

Fig. 3 shows a plot of the calculated and measured MIFR (magnitude and phase) versus $W/\lambda \cdot \cos\theta_0$. One can observe that $|g_{\perp}|$ increases, while $|g_{\parallel}|$ decreases as the gap width decreases. This effect can be explained by the fact that for parallel polarization and relatively narrow gap ($W < \lambda$) no electric field is induced in gap, while for perpendicular polarization electric field is induced in the gap due to the discontinuity in the conductive plane. This is a complementary behavior to that of a conductive strip IFR [9], which can be explained by Babinet's principle. The agreement between the calculated and measured MIFR is satisfactory for narrow gaps and diverge for

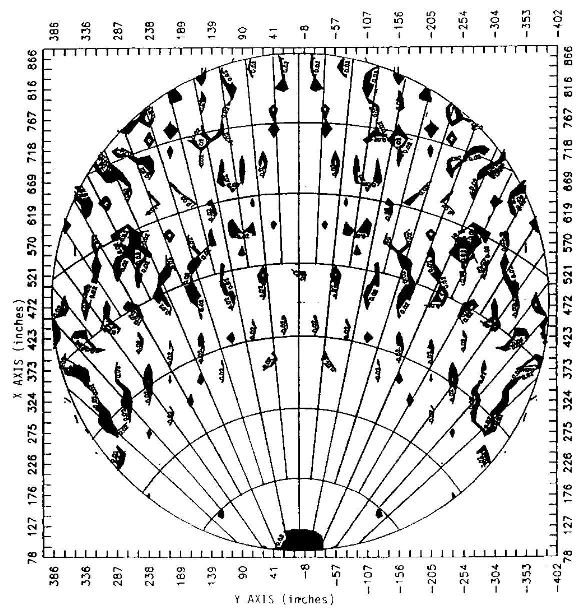


Fig. 4. Copol amplitude variation with gaps (dB) at 6 GHz.

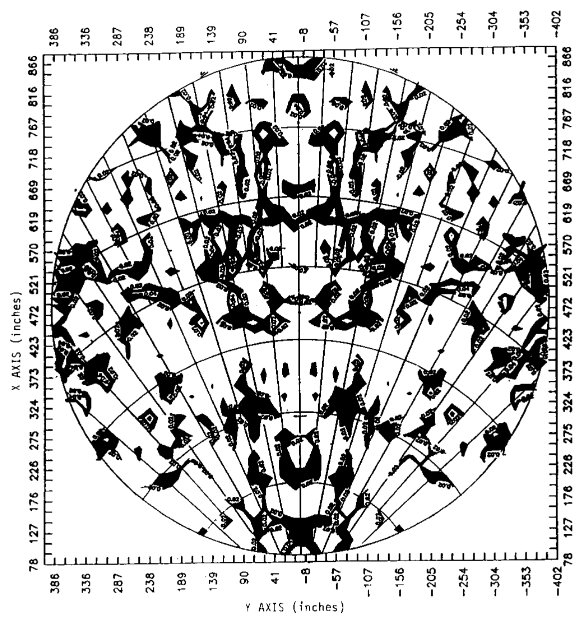


Fig. 5. Copol amplitude variation with gaps (dB) at 30 GHz.

larger gaps, when (6) and (7) do not hold anymore and a more accurate expression for the field distribution is necessary. For large gap width ($W > \lambda$), the field generated in the gap for both polarizations approaches zero in the gap center and only the diffraction effect from the edges determines the gap scattering.

As an example of the technique presented in this paper, we have considered the gap scattering effect on the quiet zone field uniformity of a large compact range assembled recently in Arizona by the cooperation between GTRI (Georgia Technology Research Institute) and ESSCO (Electronic Space Systems Corporation). The compact range is an offset parabolic reflector with a projected aperture of 67 ft, focal distance of 150 ft, and quiet zone distance of 300 ft. The angles $\theta_c$ and $\theta_0$ as shown in Fig. 1 are 2.48° and 15°, respectively. The number of gaps considered was 198, 60 mil wide and with an average length of 10 ft. The geometry of the gaps is shown in Fig. 4. We have performed the computations at two typical frequencies, 6 and 30 GHz. From Fig. 3 we can determine the MIFR's of the gaps. At 6 GHz we used $g_{\parallel} = -0.008 - j.229$ and $g_{\perp} = -0.74 + j2.42$ while at 30 GHz we used $g_{\parallel} = -0.06 - j.37$ and $g_{\perp} = -0.56 + j.67$. Figs. 4 and 5 show the copol computed amplitude variation of the electric field in the quiet zone plane at 6 and 30 GHz, respectively. The maximum amplitude variation is shown in the shaded areas. For both frequencies, the magnitude is approximately 0.075 dB but the distribution pattern of the shaded areas is different. At the higher frequency, the total shaded area is larger than at the lower frequency and more uniformly distributed across the aperture. The shaded areas are correlated to the grating lobes of the scattering pattern of the gaps. Since the grating lobes locations are inversely proportional to the gaps spacing in wavelength, we would expect more grating lobes (shaded areas) at the higher frequency as shown in Fig. 5. On the other hand, at the lower frequency since there are less grating lobes, their distribution pattern resembles the gaps (panels) geometry as shown in Fig. 4. One can identify almost one grating lobe per panel. The phase distribution due to the gap scattering is similar to the amplitude distribution but with a magnitude of 0.45°. The phase and amplitude perturbation can be approximated by an additional equivalent rms surface error to the actual surface error of the reflector. A phase variation of 0.45° is equivalent to 1.2 mil peak surface error at 6 GHz and 0.25 mil peak at 30 GHz. Based on the current technology, the peak surface error on outdoor large compact ranges is less than 18 mil, while for indoor compact ranges it is less than 4 mil. Accordingly, for outdoor applications the effect of the gaps is insignificant while for indoor applications, filling the gaps should be considered.

Computation of the x-pol field distribution in the quiet zone plane shows that the gaps introduce an x-pol scattering level of approximately −56 dB relative to the peak copol field level, which is acceptable for most compact range applications.

## IV. Conclusion

An analytical approach coupled with experimental determination of a key parameter has been developed to quantify the effect of the interpanel gap scattering in a compact range. The results show the effect of scattering on the copol and x-pol field distribution in the quiet zone area. The effect of the gap scattering can be regarded as an additional root mean square error on the antenna surface accuracy.

## Acknowledgment

The authors wish to express their thanks to Al Cohen for his encouragement and stimulating discussions in the course of this work.

## References

[1] K. Y. Kabalan *et al.*, "Characteristic modes for slots in a conducting plane, TE case," *IEEE Trans. Antennas Propagat.*, vol. AP-35, Feb. 1987.

[2] —, "Characteristic modes for a slot in a conducting plane, TM case," *IEEE Trans. Antennas Propagat.*, vol. AP-35, Mar. 1987.

[3] R. F. Millar, "A note on diffraction by an infinite slit," *Can J. Phys.*, vol. 38, pp. 38–47, 1960.

[4] T. B. A. Senior *et al.*, "Scattering by gaps and cracks," *IEEE Trans. Antennas Propagat.*, vol. 37, June 1989.

[5] D. N. Black *et al.*, "A model for the quiet zone effect of gaps in compact range reflectors," in *Proc. 1988 Antenna and Meas. Techn. Assoc. Meet.*, Atlanta, GA, Sept. 12-16, 1988, pp. 15-22.

[6] T.-S. Chu *et al.*, "Depolarization properties of offset reflector antennas," *IEEE Trans. Antennas Propagat.*, vol. AP-21, May 1973.

[7] S. Silver, *Microwave Antenna Theory and Design*. London, U.K.: Peregrinus, 1984, ch. 3, pp. 198.

[8] W. V. T. Rusch *et al.*, "Forward scattering from square cylinders in the resonance region with application to aperture blockage," *IEEE Trans. Antennas Propagat.*, vol. AP-24, Mar. 1976.

[9] P. D. Kennedy, "An analysis of the electrical characteristics of structurally supported radomes," Ohio State Univ. Rep., Contract AF-30(602)-1620, Nov. 1958.


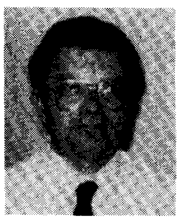

**Reuven Shavit** (M'82-SM'90) was born in Rumania on November 14, 1949. He received the B.S. and M.S. degrees in electrical engineering from the Technion, Israel, in 1971 and 1977, respectively, and the Ph.D. degree in electrical engineering from the University of California, Los Angeles, in 1982.

From 1971 to 1979 he worked with the Israeli Ministry of Defense, Tel Aviv, as a Staff Engineer and Antenna Group Leader. From 1979 to 1982 he was a Research Assistant at the University of California, Los Angeles. From 1982 to 1988 he was the Antenna Group Leader in the Electronic Research Laboratories of the Israeli Ministry of Defense, Tel Aviv, where he was involved in the design of reflector, microstrip and slot antenna arrays. He was also a part-time lecturer at Tel Aviv University, teaching various antenna and electromagnetic courses. Currently, he is with ESSCO, Concord, MA, as a Principal Engineer involved in scattering analysis and tuning techniques of high performance ground based radomes. His present research interest is in the areas of frequency selective surfaces, tuning techniques for radomes, numerical methods, reflector, microstrip and slot antenna arrays.

**Adam P. Smolski** was born in Norwood, MA, in 1925. He received the A.E.E. degree from the Lincoln Institute of Northeastern University, Boston, MA, in 1960 and the B.B.A. degree in engineering and management from the College of Business Administration, Northeastern University, in 1962.

From 1955 to 1962 he worked for the MIT Lincoln Laboratory and was responsible for the installation, operation and upgrading of the Lincoln Laboratory Antenna Test Facility. He joined the Electronic Space Systems Corporation in 1962. In his current position he is responsible for research and development projects pertaining to low-loss sandwich-type radomes. He is also responsible for all electromagnetic testing of antennas and radomes at the ESSCO Antenna Test Facility in Concord, MA.

Mr. Smolski is a member of Sigma Epsilon Rho.

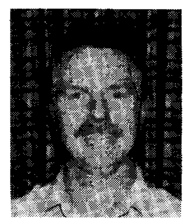

**Crit J. Cook** (M'87) received the B.S. degree in physics from Sam Houston State University, Huntsville, TX, in 1984. He continued graduate studies there, and also in electrical engineering at Southern Methodist University, Dallas, TX.

He was Antenna Design Engineer at Texas Instruments through 1987, Electromagnetic Engineer at ESSCO through 1990, and is currently Engineering Group Leader at AFC-Microdyne in Ocala, FL, doing electromagnetic scattering design of radomes and antennas. His technical interests are the numerical techniques in electromagnetic scattering and bistatic test methods.